A Finite Difference Polar-Cartesian Grid Approach for Mode Computation in Rounded-End Waveguides

Alessandro Fanti and Giuseppe Mazzarella

Department of Electrical and Electronic Engineering
University of Cagliari, 09123, Piazza d'Armi, Cagliari, Italy
alessandro.fanti@diee.unica.it, mazzarella@diee.unica.it

Abstract ─ A finite-difference technique to compute Eigenvalues and mode distribution of non standard waveguide (and aperture) is presented. It is based on a mixed mesh (Cartesian-polar) to avoid staircase discretization of curved edges, and is able to give accuracy comparable to FEM and FIT techniques with a reduced computational burden.

Index Terms ─ Eigenvalue, finite-difference, Helmholtz equation, waveguide modes.

I. INTRODUCTION

In finite difference time domain (FDTD) analysis of waveguide components, the knowledge of the modal expansion can reduce significantly the computation time, since it is possible to model each homogeneous waveguide trunk as a (small) set of 1D-FDTD problems [1]. This approach, however, requires the waveguide mode functions be known, either analytically, or numerically but on a grid matched to the 3D FDTD grid used in the inhomogeneous regions.

The same knowledge of mode function is useful in the analysis of waveguide junction using mode matching [2-6], solution of waveguide problems with sources [7], and the method of moments (MOM) analysis of thick-walled waveguide slot for linear [8] and circular polarization [9] and for apertures [10].

Apart from some simple geometries, mode computation cannot be done in closed forms, so that suitable numerical techniques must be used. Among them, finite difference (FD) techniques [11], despite of their long history, are still very popular both for their simplicity and computational effectiveness.

The most popular FD approach is based on the use of a standard four-point FD approximation [12] of the Laplace operator. But it requires a rectangular discretization grid, and therefore a boundary with all sides parallel to the rectangular axes. As a consequence, many geometries cannot be dealt with exactly with this approach, requiring a staircase approximation of the boundaries.

The aim of this paper is to present a FD technique for the computation of modes and eigenvalues of a waveguide whose boundary consists of segments and circular arcs, taking exactly into account the curved boundary of the waveguide and with no loss of accuracy. Among those waveguides, rounded-end rectangular waveguides (Fig. 1) are the most interesting, and will be detailed here for the technique assessment. Our approach, which uses a polar grid for the curved region and a rectangular grid for the straight ones, is not limited to rounded-end rectangular waveguides, but can be straight forwardly extended to many other geometries.

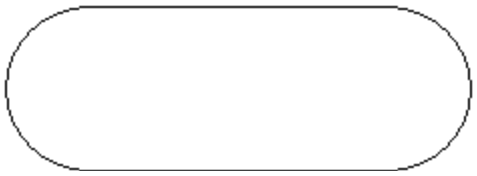

Fig. 1. Rounded-end rectangular waveguide.

This approach can be used for circular waveguides too, and the following case starts with a two-fold purpose: first, to describe the main part of our approach in a simpler way; second, to set up a test-bench to assess our approach. As a matter of fact, we will compare the results of our approach on non-standard waveguides with a commercial, general-purpose, software. The accuracy of this

Submitted On: May 31, 2011
Accepted On: October 8, 2011

software, compared to our approach, will be tested in the circular case, where the exact solution is known.

The comparison presented shows that the technique proposed here gives results comparable to those obtained with the finite element method (FEM) and the finite integration technique (FIT) [13], but with a lower computational cost.

II. DESCRIPTION OF THE TECHNIQUE

A. Technique framework

Let us consider a generic waveguide. TE modes can be found [7] from a suitable scalar eigenfunction φ, solution of the Helmholtz equation:

$$\nabla_t^2\varphi + k_t^2\varphi = 0, \tag{1}$$

with the boundary condition (BC)

$$\frac{\partial\varphi}{\partial n} = 0, \tag{2}$$

at the boundary of the waveguide. In the FD approach both the equation (1) and the BC (2) are replaced by a discretised version, i.e., replacing derivatives with finite approximations. This transform (1) into a matrix eigenvalue problem, whose eigenvectors contain the samples of φ at the discretization nodes. The matrix is sparse, so a very effective computation is possible.

If the waveguide boundary consists of straight lines, parallel to the coordinate axes, the FD method can be applied on a Cartesian grid [12]. This grid defines also a partition of the waveguide surface into rectangular cells, which completely fill the waveguide section. For every other waveguide, the section cannot be exactly partitioned using rectangular cells and this leads to numerical errors (since the eigenvalue problem is quite ill – conditioned [14]).

In order to get a high accuracy, the waveguide surface must be discretized maintaining also the correct geometry of the boundary. So a different discretization scheme should be used, which matches exactly the waveguide boundary. Therefore, the discretization nodes must be at the intersections of a suitable framework, in which the waveguide boundary is a coordinate curve. In this way, the waveguide section is exactly partitioned into a discretization cell.

The discretized equations can be obtained in two ways. The standard approach is to sum a Taylor expansion of the potentials [12]. Alternatively, we can integrate (1) over a discretization cell [11]

$$\int \nabla_t^2\varphi dS = -k_t^2 \int \varphi dS\,. \tag{3}$$

Use of the Gauss theorem then gives:

$$\int_{\Gamma_F} \nabla_t^2\varphi \cdot i_n dl = -k_t^2 \int_{S_F} \varphi dS\,, \tag{4}$$

i.e.

$$\int_{\Gamma_F} \frac{\partial\varphi}{\partial n}\cdot dl = -k_t^2\varphi\,, \tag{5}$$

where Γ_F is the cell boundary, S_F is the cell surface and φ is evaluated at the discretization node in the right hand side. The left hand side of (5) is then divided into four (or more) sides, along the coordinate curves, and the normal derivative is evaluated in finite terms.

The two approaches apply in non-overlapping sets of cases, but when both can be used, the results are the same, as we will show later.

Since both discretizations (either the standard FD and that based on (5)) can easily include the BC (2), the resulting FD formulation to equivalent to the complete eigenvalue problem (1,2).

B. Circular waveguide

In order to explain the difference with the standard FD, and to assess our approach, we start considering a circular waveguide (see Fig. 2), using as grid lines the coordinate lines of a polar framework. We assume a regular spacing on the coordinate lines, with step Δr, $\Delta\vartheta$, and let $\varphi_{nq} = \varphi(n\Delta r, q\Delta\vartheta)$.

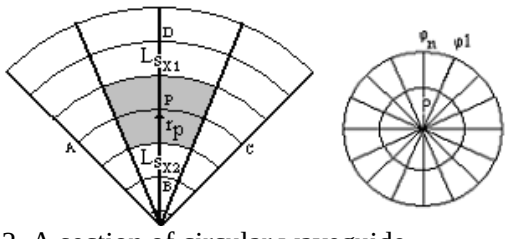

Fig. 2. A section of circular waveguide.

Let P the point of coordinates $(n\Delta r, q\Delta\vartheta)$, and consider the four nearby points A, B, C, and D, as shown in Fig. 2. For the left hand side of (5), we get

$$\frac{1}{S_F}\cdot\left[\frac{(\varphi_D-\varphi_P)}{\Delta r}\cdot L_{Sx1}+\frac{(\varphi_B-\varphi_P)}{\Delta r}\cdot L_{Sx2}+\right.$$
$$\left.+\frac{(\varphi_A-\varphi_P)}{\Delta\vartheta\cdot r_p}\cdot\Delta r+\frac{(\varphi_C-\varphi_P)}{\Delta\vartheta\cdot r_p}\cdot\Delta r\right], \quad (6)$$

where $S_F=r_P\cdot\Delta r\cdot\Delta\vartheta$, $L_{SX1}=\left(r_P+\frac{\Delta r}{2}\right)\cdot\Delta\vartheta$ and

$$L_{SX2}=\left(r_P-\frac{\Delta r}{2}\right)\cdot\Delta\vartheta.$$

Replacing and collecting the term, we get the discretized form of (1) as:

$$\frac{1}{r_p^2(\Delta\vartheta)^2}\cdot\varphi_A+\left(\frac{1}{2r_p\Delta r}+\frac{1}{(\Delta r)^2}\right)\cdot\varphi_D+$$
$$+\frac{1}{r_p^2(\Delta\vartheta)^2}\cdot\varphi_C+\left(\frac{1}{(\Delta r)^2}-\frac{1}{2r_p\Delta r}\right)\cdot\varphi_B+ \quad (7)$$
$$-\left(\frac{2}{(\Delta r)^2}+\frac{2}{r_p^2(\Delta\vartheta)^2}\right)\cdot\varphi_P\cong-k_t^2\varphi_p^2$$

This expression can be used for all internal points, except the circle centre.

It is worth noting that (8) can be obtained also starting from the Helmholtz equation in polar coordinates.

$$\left[\frac{1}{r_p^2}\cdot\frac{\partial^2\varphi}{\partial\vartheta^2}+\frac{1}{r_p}\cdot\frac{\partial\varphi}{\partial r}+\frac{\partial^2\varphi}{\partial r^2}\right]=-k_t^2\varphi, \quad (8)$$

and using a Taylor approximation.

$$\varphi_B=\varphi_P+\left.\frac{\partial\varphi}{\partial r}\right|_P\cdot(-\Delta r)+\frac{1}{2}\left.\frac{\partial^2\varphi}{\partial r^2}\right|_P\cdot(-\Delta r)^2, \quad (9)$$

$$\varphi_D=\varphi_P+\left.\frac{\partial\varphi}{\partial r}\right|_P\cdot(+\Delta r)+\frac{1}{2}\left.\frac{\partial^2\varphi}{\partial r^2}\right|_P\cdot(+\Delta r)^2. \quad (10)$$

Adding and subtracting the last two equations we find:

$$\left.\frac{\partial^2\varphi}{\partial r^2}\right|_P=\frac{1}{(\Delta r)^2}\cdot(\varphi_B+\varphi_D-2\varphi_P), \quad (11)$$

and

$$\left.\frac{\partial\varphi}{\partial r}\right|_P=\frac{\phi_D-\varphi_B}{2\cdot\Delta r}. \quad (12)$$

Likely in ϑ direction

$$\left.\frac{\partial^2\varphi}{\partial\vartheta^2}\right|_P=\frac{1}{(\Delta\vartheta)^2}\cdot(\varphi_A+\varphi_C-2\varphi_P). \quad (13)$$

Collecting all those equation in (8) we get (7). It remains to consider the last point, i.e. the centre of the circle. In this point, it is not possible to use a Taylor expression since it is a point of singularity. So we are forced to use (5).

The left hand side of (5) can be expanded as (see Fig. 2)

$$\left(\frac{1}{\pi\cdot\left(\frac{\Delta r}{2}\right)^2}\right)\cdot\sum_{q=1}^{N}\frac{(\varphi_q-\varphi_P)}{\Delta r}\cdot\frac{\Delta r}{2}\cdot\Delta\vartheta, \quad (14)$$

and therefore the discretized form of the equation (1) is:

$$\left(\frac{4}{\pi\cdot\Delta r^2}\right)\cdot\left(\sum_{q=1}^{N}\varphi_q\frac{\Delta\vartheta}{2}-N\frac{\Delta\vartheta}{2}\varphi_P\right)\cong-k_t^2\varphi_P. \quad (15)$$

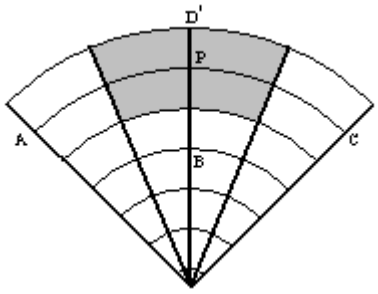

Fig. 3. Boundary point of circular waveguide.

On the boundary points in Fig. 3, for TE modes we can replace (9) by a first-order approximation

$$\varphi_P=\varphi_D+\left.\frac{\partial\varphi}{\partial r}\right|_D\cdot\left(\frac{\Delta r}{2}\right)$$ and since the BC is $\left.\frac{\partial\varphi}{\partial r}\right|_D=0$, we get $\varphi_P=\varphi_D$.

As a consequence (11) becomes:

$$\left.\frac{\partial^2\varphi}{\partial r^2}\right|_P=\frac{1}{\Delta r^2}\cdot(\varphi_B-\varphi_P), \quad (16)$$

and (7) is replaced by:

$$\frac{1}{r_p^2\Delta\vartheta^2}\cdot\varphi_A+\frac{1}{r_p^2\Delta\vartheta^2}\cdot\varphi_C+$$
$$+\left(\frac{1}{\Delta r^2}-\frac{1}{2r_p\Delta r}\right)\cdot\varphi_B+ \quad . \quad (17)$$
$$-\left(\frac{1}{\Delta r^2}-\frac{1}{2r_p\Delta r}+\frac{2}{r_p^2\Delta\vartheta^2}\right)\cdot\varphi_P\cong-k_t^2\varphi_p$$

C. Rounded-end waveguide

Now consider the section of a rounded-end waveguide (see Fig. 4). The section can be divided into three regions. In the external ones, we use a polar framework; while in the central one, we can use the standard Cartesian framework, as in Fig. 4.

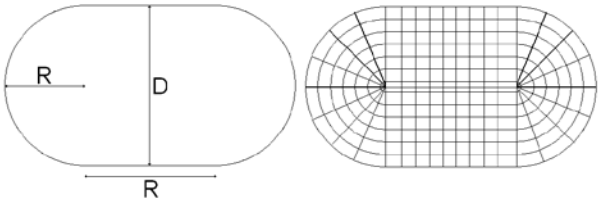

Fig. 4. A mixed mesh (Cartesian-polar) of non-standard waveguide and its dimensions.

In the Cartesian framework, we assume a regular spacing on the coordinate lines, with step $\Delta x,\Delta y$ (see Fig. 4).

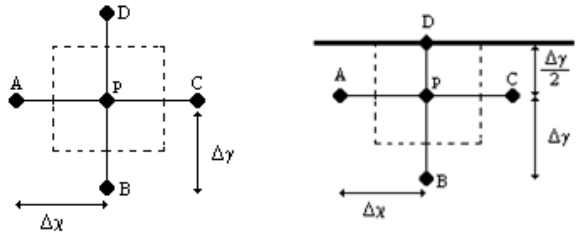

Fig. 5. (a) Internal point , (b) boundary point .

For each internal point, we can use the standard expression of the Laplacian obtained by the Taylor expansion [10]:

$$\nabla_t^2\varphi_p=\frac{\varphi_A}{\Delta x^2}+\frac{\varphi_C}{\Delta x^2}+\frac{\varphi_B}{\Delta y^2}+\frac{\varphi_D}{\Delta y^2}+$$
$$+\left(\frac{2}{\Delta x^2}+\frac{2}{\Delta y^2}\right)\varphi_P \quad , \quad (18)$$

and replace (1) by the discretized form:

$$\frac{\varphi_{i,j-1}}{\Delta x^2}+\frac{\varphi_{i,j+1}}{\Delta x^2}+\frac{\varphi_{i-1,j}}{\Delta y^2}+\frac{\varphi_{i+1,j}}{\Delta y^2}+$$
$$+\left(\frac{2}{\Delta x^2}+\frac{2}{\Delta y^2}\right)\varphi_{i,j}=-k_t^2\varphi_{i,j} \quad . \quad (19)$$

Equation (19) cannot be used for boundary points, where BC (2) must be enforced. For a boundary point, using 3 nearby points, A,B,C, in Fig. 5b, we get:

$$\frac{\varphi_A}{\Delta x^2}+\frac{\varphi_C}{\Delta x^2}+\frac{\varphi_B}{\Delta y^2}+\left(\frac{2}{\Delta x^2}+\frac{1}{\Delta y^2}\right)\varphi_P=$$
$$-k_t^2\varphi_P \quad , \quad (20)$$

and analogously one can do the same to (17). In the polar regions, we use the expression (7) and (17), so it remains to analyze the border between the polar and the Cartesian regions, Fig. 6. Since the grid geometry here is not a regular one, a new approximation of the Laplacian operator must be used, tailored to the geometry at hand. We propose here a general approach to derive such approximations in unusual geometries, which can be easily extended to discretize other differential operators.

For each point (except the centre), let us number with 0 the sampling point, and with i (i = 1, . . . , 5) its neighbouring points as in Fig. 6a. The discretized form of $\nabla_t^2\varphi$ can always be written as:

$$\nabla_t^2\phi=\frac{\partial^2\phi}{\partial x^2}+\frac{\partial^2\phi}{\partial y^2}\cong\sum_i A_i\left(\varphi_i-\varphi_0\right). \quad (21)$$

Each difference in (21) can be expressed as a Taylor series:

$$\varphi_i-\varphi_0=\left.\frac{\partial\varphi}{\partial x}\right|_0\cdot\Delta x_i+\left.\frac{\partial\varphi}{\partial y}\right|_0\cdot\Delta y_i+$$
$$+\frac{1}{2}\left.\frac{\partial^2\varphi}{\partial x^2}\right|_0\cdot\Delta x_i^{\,2}+\frac{1}{2}\left.\frac{\partial^2\varphi}{\partial y^2}\right|_0\cdot\Delta y_i^{\,2}+, \quad (22)$$
$$+\left.\frac{\partial^2\varphi}{\partial x\partial y}\right|_0\cdot\Delta x_i\cdot\Delta y_i$$

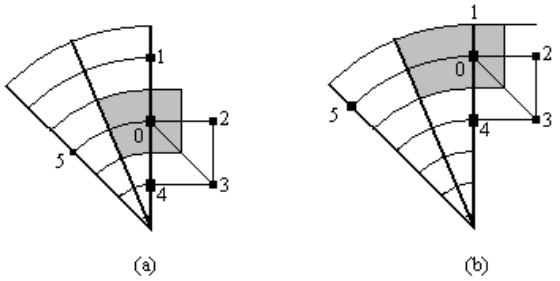

Fig. 6. (a) Point between polar and Cartesian framework. (b) Boundary point between polar and Cartesian framework.

where all derivatives of φ are computed at the sampling point, and $(\Delta x_i, \Delta y_i)$ is the position of the i–th point w.r.t point 0.

Using (21), the right hand side of (22) becomes:

$$B_1\frac{\partial\varphi}{\partial x}+B_2\frac{\partial\varphi}{\partial y}+B_3\frac{\partial^2\varphi}{\partial x^2}+B_4\frac{\partial^2\varphi}{\partial y^2}+B_5\frac{\partial^2\varphi}{\partial x\partial y}, \quad (23)$$

where B_i in (23) are linear combination of the unknown coefficient A_i.

$$\begin{aligned}
B_1 &= A_1\Delta x_1 + A_2\Delta x_2 + A_3\Delta x_3 + A_4\Delta x_4 + A_5\Delta x_5\\
B_2 &= A_1\Delta y_1 + A_2\Delta y_2 + A_3\Delta y_3 + A_4\Delta y_4 + A_5\Delta y_5\\
B_3 &= A_1\Delta x_1^2 + A_2\Delta x_2^2 + A_3\Delta x_3^2 + A_4\Delta x_4^2 + A_5\Delta x_5^2\\
B_4 &= A_1\Delta y_1^2 + A_2\Delta y_2^2 + A_3\Delta y_3^2 + A_4\Delta y_4^2 + A_5\Delta y_5^2\\
B_5 &= A_1\Delta x_1\Delta y_1 + A_2\Delta x_2\Delta y_2 + A_3\Delta x_3\Delta y_3 +\\
&+A_4\Delta x_4\Delta y_4 + A_5\Delta x_5\Delta y_5
\end{aligned} \quad (24)$$

Equation (23) is a second order approximation of the Laplace operator if

$$B_1 = B_2 = B_5 = 0 \qquad B_3 = B_4 = 1, \quad (24)$$

which is a linear system in the A_i. Its solution gives the required coefficient of (2).

For a boundary point see Fig. 6b, boundary condition (2) can be expressed as:

$$\alpha_1\left.\frac{\partial\varphi}{\partial x}\right|_1+\alpha_2\left.\frac{\partial\varphi}{\partial y}\right|_1=0, \quad (25)$$

where α_1, α_2 are the components of a unit vector normal to the boundary, (25) can be used to replace equations $B_1 = B_2 = 0$ with a single one, to compensate for the absence of one unknown (see Fig. 6b).

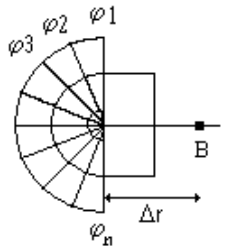

Fig. 7. Centre point between polar and Cartesian framework

For the centre of the circle, see Fig. 7, we still use (5) to get:

$$\left(\frac{8}{\pi\Delta r^2}\right)\cdot\sum_{q=1}^{N}\frac{(\varphi_q-\varphi_P)}{\Delta r}\cdot\frac{\Delta r}{2}\cdot\Delta\vartheta+$$
$$+\left(\frac{2}{\Delta r^2}\right)\cdot\left(\frac{(\varphi_1+\varphi_N)}{2}+\varphi_B-2\varphi_P\right)=-k_t^2\varphi_P \quad (26)$$

Putting together all equations, we get a matrix eigenvalue problem [14] whose solution gives the required waveguide modes.

III. NUMERICAL EXPERIMENTS

The discretized eigenvalues problem obtained in the last section must be solved by a numerical routine. As a matter of fact, a highly sparse matrix is obtained, so that the sparse matrix routines of Matlab have been used. We have first compared the first few TE eigenvalues for a circular waveguide with analytical results and with a FIT simulation performed with CST.

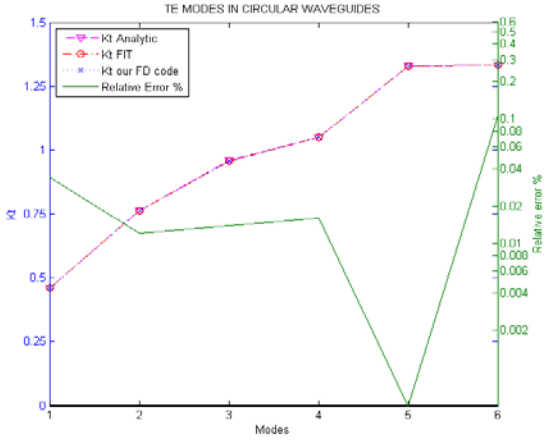

Fig. 8. Comparison between our FD code and analytic results and FIT(CST) results for TE modes in circular wave guide with r=4 mm Δr =0.0792 mm and ϑ=1°.

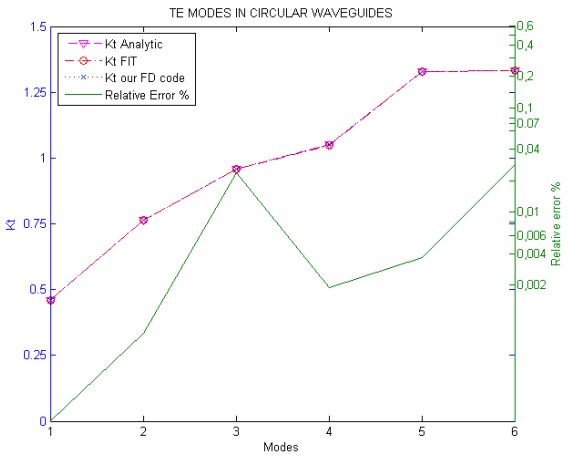

Fig. 9. Comparison between our FD code and analytic results and FIT(CST) results for TE modes in circular wave guide with r=4 mm Δr =0.0792 mm and $\Delta\vartheta$=0,5°.

We have made several tests by varying the steps (Δr, $\Delta\vartheta$). The results of Figs. 8 and 9 show that our technique has a very low error, as long as the steps are small.

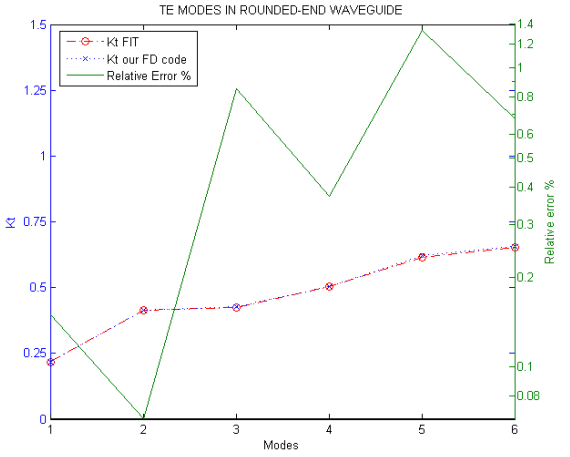

Fig. 10. Comparison between our FD code and FIT (CST) results for TE modes in rounded-end wave guide with $\Delta x = \Delta y = \Delta r = 0{,}1569$ mm D=B=8 mm and ϑ=1°.

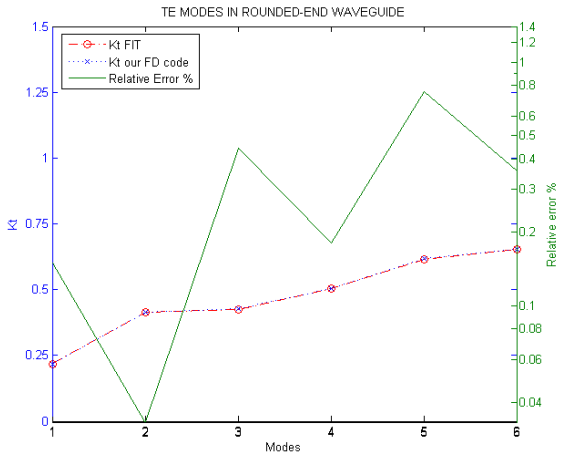

Fig. 11. Comparison between our FD code and FIT (CST) results for TE modes in rounded-end wave guide with $\Delta x = \Delta y = \Delta r = 0{,}0792$ mm D=B=8 mm and $\Delta\vartheta$=1°.

When compared to CST, our results are better, and can be obtained in a fraction of the computational time required by the former. However, the comparison of FIT and analytical results show that the CST is quite accurate, too, and can be used to test our approach for the rounded-end waveguide.

To assess our FD code in this case, we have evaluated a few TE modes, for different structures (see Figs. 10 - 15). Figures 10 – 15 show the comparison between our results and CST ones.

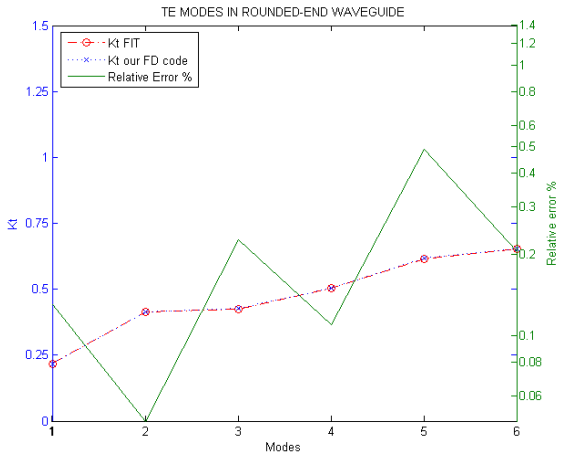

Fig. 12. Comparison between our FD code and FIT (CST) results for TE modes in rounded-end wave guide with $\Delta x = \Delta y = \Delta r = 0{,}03980$ mm D=B=8 mm and ϑ=1°.

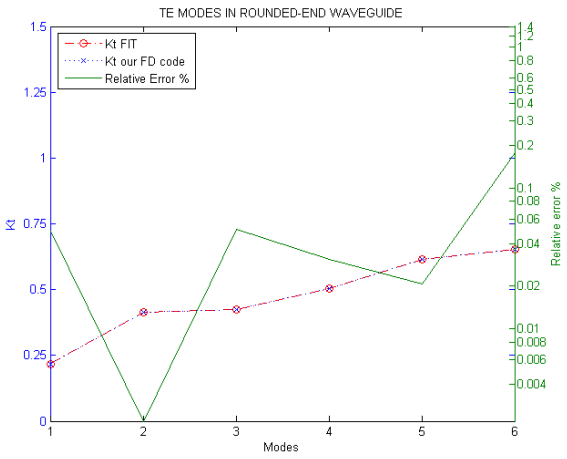

Fig. 13. Comparison between our FD code and FIT (CST) results for TE modes in rounded-end wave guide with $\Delta x = \Delta y = \Delta r = 0{,}01995$ mm D=B=8 mm and ϑ=1°.

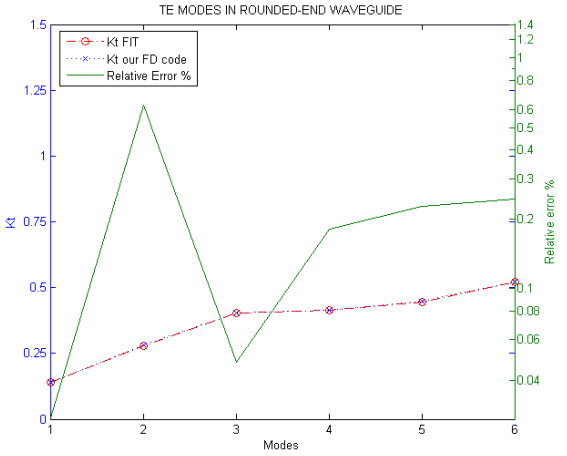

Fig. 14. Comparison between our FD code and FIT (CST) results for TE modes in rounded-end wave guide with $\Delta x = \Delta y = \Delta r =$ 0,0792 mm D=8 mm B=16 mm and ϑ=1°.

The results show that our FD approach allows a high accuracy, when the discretization step is suitably chosen. But even a quite large area, such as in Table 3, allows a quite accurate mode evaluation.

VI. CONCLUSION

A FD approach to the computation of the TE modes of the waveguide using a mixed polar-Cartesian grid has been described. The typical sparse matrix obtained by the FD allows an effective computation of the eigenvalues, with a good accuracy, as shown by our tests. The described approach can be extended to waveguides with more general geometries, as long as the guide boundary is a coordinate curve of a suitable framework.

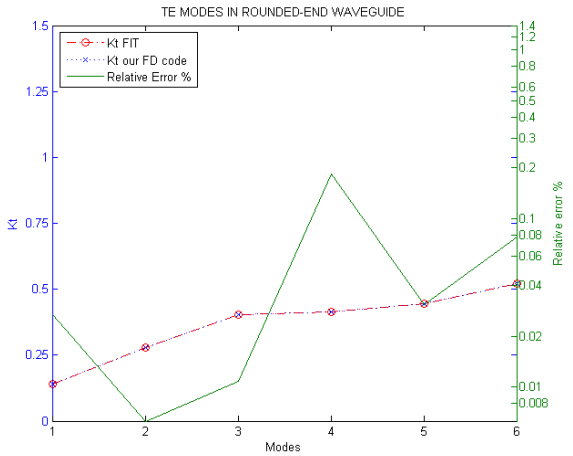

Fig. 15. Comparison between our FD code and FIT (CST) results for TE modes in rounded-end wave guide with $\Delta x = \Delta y = \Delta r =$ 0,03980 mm D=8 mm B=16 mm and ϑ=1°.

REFERENCES

[1] F. Alimenti, P. Mezzanotte, L. Roselli, and R. Sorrentino, “Efficient Analysis of Waveguide Components by FDTD Combined with Time Domain Modal Expansion,” *MGWL*, vol. 5, pp. 351-353, October 1995.

[2] A. Wexler, “Solution of Waveguide Discontinuities by Modal Analysis,” *IEEE Trans. Microwave Theory and Techniques*, vol. MTT-15, pp. 508-517, September 1967.

[3] A. Pellegrini, S. Bertini, A. Monorchio, and G. Manara, “A Mode Matching - Finite Element - Spectral Decomposition Approach for the Analysis of Large Finite Arrays of Horn Antennas,” *Applied Computational Electromagnetic Society (ACES) Journal*, vol. 24, no. 2, pp. 233–240, April 2009.

[4] K. L. Chan and S. R. Judah, “Mode-Matching Analysis of a Waveguide Junction Formed by a Circular and a Larger Elliptic Waveguide,“ *IEEE Trans. Microwaves, Antennas and Propagation, IEE Proceedings*, vol. 145, pp. 123 - 127, February 1998.

[5] S. L. Lin, L. W. Li, T. S. Yeo, and M. S. Leong, "Novel Unified Mode Matching Analysis of Concentric Waveguide Junctions," *IEEE Trans. on Antennas and Propagation*, vol. 148, no. 6, pp. 369–374, December 2001.

[6] R. Sorrentino, F. Alessandri, M. Mongiardo, G. Avitabile, and L. Roselli, "Full-Wave Modeling of Via Hole Grounds in Microstrip by Three-Dimensional Mode Matching Technique," *IEEE Trans. Microwave Theory and Techniques*, vol. MTT-40, no.12, pp. 2228-2234, December 1992.

[7] R. E. Collin, *Field Theory of Guided Waves*, 2nd ed, IEEE Press, N.Y., 1991.

[8] G. Mazzarella and G. Montisci, "A Rigorous Analysis of Dielectric-Covered Narrow Longitudinal Shunt Slots with Finite Wall Thickness," *Electromagnetics*, vol. 19, pp. 407-418, October 1999.

[9] G. Montisci, M. Musa, and G. Mazzarella, "Waveguide Slot Antennas for Circularly Polarized Radiated Field," *IEEE Trans. on Antennas and Propagation*, vol. 52, pp. 619-623, Feb. 2004.

[10] G. Mazzarella and G. Montisci, "Accurate Characterization of the Interaction between Coupling Slots and Waveguide Bends in Waveguide slot Arrays," *IEEE Trans. Microwave Theory and Techniques*, vol. 48, issue 7, pp. 1154-1157, July 2000.

[11] K. W. Morton and D. F. Mayers, *Numerical Solution of Partial Differential Equations: An Introduction*, Cambridge University Press, 2005.

[12] M. J. Beaubien and A. Wexler, "An Accurate Finite-Difference Method for Higher Order Waveguide Modes," *IEEE Trans. Microwave Theory and Techniques*, vol. MTT-16, no. 12, pp. 1007-1017, December 1968.

[13] U. V. Rienen, "Triangular Grids: A Review of Resonator and Waveguide Analysis with Classical FIT and Some Reflections on Yee-like FIT- and FEM-Schemes," *Applied Computational Electromagnetic Society (ACES) Journal*, vol. 19, no. 1, pp. 73–83, March 2004.

[14] G. H. Golub and C. F. Van Loan, *Matrix Computation*, Johns Hopkins Univ. Press, 1989.

Alessandro Fanti graduated in Electronic Engineering at the University of Cagliari on 2006 and currently is a Ph.D. student in Electronic Engineering and Informatics at University of Cagliari. His research activity involves the use of numerical techniques for modes calculation in of guiding structures or in microwaves circuits.

Giuseppe Mazzarella graduated Summa with Laude in Electronic Engineering from the Università "Federico II" of Naples in 1984 and obtained the Ph.D. in Electronic Engineering and Computer Science in 1989. In 1990, he became Assistant Professor at the Dipartimento di Ingegneria Elettronica at the Università "Federico II" of Naples. Since 1992, he is with the Dipartimento di Ingegneria Elettrica ed Elettronica of the Università di Cagliari, first as associate professor and then, since 2000, as full professor, teaching courses in Electromagnetics, Microwave, Antennas and Remote Sensing. His research activity has focused mainly on: efficient synthesis of large arrays of slots, power synthesis of array factor, with emphasis on inclusion of constraints, microwave holography techniques for the diagnosis of large reflector antennas, use of evolutionary programming for inverse problems solving, in particular problems of synthesis of antennas and periodic structures. He is author (or co-author) of about 40 papers in international journals, and is a reviewer for many EM journals.